



OPEN

Inactivation of TRPM7 kinase activity does not impair its channel function in mice

SUBJECT AREAS:

ION CHANNEL
SIGNALLING

KINASES

ION CHANNELS

Taku Kaitsuka^{1,2*}, Chiaki Katagiri^{1,3*}, Pavani Beesetty⁴, Kenji Nakamura¹, Siham Hourani⁴, Kazuhito Tomizawa², J. Ashot Kozak⁴ & Masayuki Matsushita^{1,3}Received
7 April 2014Accepted
23 June 2014Published
17 July 2014Correspondence and
requests for materials
should be addressed to
M.M. (masayuki@
med.u-ryukyu.ac.jp)* These authors
contributed equally to
this work.

¹Mitsubishi Kagaku Institute of Life Sciences, Machida, Tokyo 194-8511, Japan, ²Department of Molecular Physiology, Faculty of Life Sciences, Kumamoto University, Kumamoto 860-8556, Japan, ³Department of Molecular and Cellular Physiology Graduate School of Medicine, University of the Ryukyus, 903-0215 Okinawa, Japan, ⁴Department of Neuroscience, Cell Biology and Physiology, Wright State University, Dayton, OH 45435, USA.

Transient receptor potential (TRP) family channels are involved in sensory pathways and respond to various environmental stimuli. Among the members of this family, TRPM7 is a unique fusion of an ion channel and a C-terminus kinase domain that is highly expressed in immune cells. TRPM7 serves as a key molecule governing cellular Mg²⁺ homeostasis in mammals since its channel pore is permeable to Mg²⁺ ions and can act as a Mg²⁺ influx pathway. However, mechanistic links between its kinase activity and channel function have remained uncertain. In this study, we generated kinase inactive knock-in mutant mice by mutagenesis of a key lysine residue involved in Mg²⁺-ATP binding. These mutant mice were normal in development and general locomotor activity. In peritoneal macrophages isolated from adult animals the basal activity of TRPM7 channels prior to cytoplasmic Mg²⁺ depletion was significantly potentiated, while maximal current densities measured after Mg²⁺ depletion were unchanged in the absence of detectable kinase function. Serum total Ca²⁺ and Mg²⁺ levels were not significantly altered in kinase-inactive mutant mice. Our findings suggest that abolishing TRPM7 kinase activity does not impair its channel activity and kinase activity is not essential for regulation of mammalian Mg²⁺ homeostasis.

TRPM7 is a member of the transient receptor potential (TRP) family of cation channels, displaying outward rectification and permeable to a number of divalent metal ions, including Mg²⁺ and Ca²⁺¹⁻⁴. A closely related gene, TRPM6, was identified as being mutated in familial hypomagnesemia with secondary hypocalcemia^{5,6}, and a key role for both TRPM6 and TRPM7 has been suggested in cellular Mg²⁺ homeostasis⁵⁻¹⁰. TRPM7 channel is widely expressed, with particularly high numbers of functional channels in immune cells and cardiac and smooth muscle cells^{1,4,7,11,12}. A hallmark of TRPM7 channels is their sensitivity to cytoplasmic Mg²⁺^{1,2}. Using patch-clamp electrophysiology, we recently demonstrated that inhibition by Mg²⁺ is biphasic, with ~10 μM and ~165 μM IC₅₀ values¹². Interestingly, Mg²⁺ sensitivity of TRPM7 channels is not constant but increases with multiple Mg²⁺ applications to inside-out patches¹³. In addition to Mg²⁺, TRPM7 is also inhibited by other metal cations Zn²⁺, Mn²⁺, Ca²⁺ and polyvalent cations such as spermine or neomycin¹⁴. Both native (endogenous) and heterologously expressed TRPM7 can be activated by cytoplasmic alkalization and inhibited by acidification¹⁴. We determined that intracellular pH dependence of native human TRPM7 channels is monophasic with an IC₅₀ of pH 6.3¹².

TRPM7 channels are expressed in mammalian cell lines commonly used for heterologous gene expression, such as HEK293 and CHO-K1^{2,12,15}. This presents a problem in studies of TRPM7 kinase function since the background kinase activity existing in these cell lines may reduce the effects of introducing inactivating kinase mutations. The TRPM7 kinase-dead knock-in mouse model, therefore, would allow us to study TRPM7 channel activity a) in its native environment at physiological expression levels, and b) in the complete absence of kinase activity.

TRPM7 is a unique protein that contains an atypical kinase domain at its C-terminus, closely similar to eukaryotic elongation factor-2 kinase (eEF2K)¹⁶⁻¹⁹. This kinase is reported to have several substrates *in vitro*, such as TRPM7 itself, annexin A1, phospholipase Cγ2 (PLCγ2) and eEF2K^{15,20-22}. The TRPM7 kinase domain plays a structural role and is essential for ion channel activity^{8,10,15}. Deletion of the kinase domain resulted in significantly reduced TRPM7 currents and increased sensitivity to Mg²⁺^{8,10,15}. However, the role of the kinase activity and autophosphorylation in the ion channel function remains controversial^{8,14,15,16,23}. In some reports, the



kinase activity was shown to affect the channel function^{8,16,23}, while others showed that kinase activity did not change channel current amplitudes or sensitivity to high concentrations of Mg^{2+} ¹⁵. This discrepancy could be caused by the use of heterologous expression of TRPM7 mutants or by deletion of the kinase domain.

In the present study, to address if TRPM7 kinase activity has any roles in channel function, we generated kinase-inactive mutant mice and analyzed their phenotype and channel activity. Our results clearly show that kinase activity of TRPM7 is not required for the native channel function. In macrophages isolated from kinase-inactive mutant animals the basal TRPM7 channel activity was increased yet maximal activity was not significantly changed. We also found that the mutant mice exhibited normal development and serum total Mg^{2+} and Ca^{2+} concentrations. Our findings suggest that TRPM7 kinase activity is dissociated from its channel activity and regulation of mammalian Mg^{2+} homeostasis.

Results

Generation of the TRPM7 kinase-dead mutant mouse. We generated TRPM7 kinase-inactive mutant mice by homologous recombination in embryonic stem (ES) cells to replace the wild-type (WT) *Trpm7* gene with a point mutant *Trpm7* allele encoding TRPM7 K1646R protein. The construct of targeting vector is shown in Figure 1A. K1646 is equivalent to the conserved lysine residue of classical kinases that is often mutated to produce a kinase-inactive protein, and its mutation to arginine results in diminished kinase activity¹⁵. After homologous recombination in ES cells, heterozygotes were confirmed by Southern blot analysis (Fig. 1B). Subsequently, heterozygote mice were generated using standard procedures. Deletion of the neo cassette was performed by microinjection of pCAGGS-Cre into pronuclei of fertilized eggs derived from heterozygous mice²⁴, and confirmed by Southern blot analysis (Fig. 1C). Homozygous “kinase-dead” mice expressing TRPM7 K1646R were obtained by breeding between heterozygous males and females; they will hereafter be referred to as TRPM7^{R/R} animals. The scheme of PCR genotyping is shown in Fig. 1D: using this PCR product, we confirmed the presence of the desired point mutation in the genomes of mice by DNA sequencing (Fig. 1E).

TRPM7^{R/R} mice display normal development and serum Mg^{2+} levels. In order to investigate key physiological characteristics of TRPM7^{R/R} mice, we performed biochemical analysis of the serum total Mg^{2+} and Ca^{2+} levels. TRPM7^{R/R} mice had normal serum total Mg^{2+} and Ca^{2+} levels (Fig. 2A). Under standard conditions, growth and viability was normal in TRPM7^{R/R} mice that were followed up for ~10 months, and there were no remarkable differences in body weight, food intake or locomotor activity between WT and TRPM7^{R/R} animals (Fig. 2B–D).

TRPM7^{R/R} mice have greatly diminished kinase activity. To determine if the kinase activity of TRPM7 was abolished in TRPM7^{R/R} mice, we analyzed the phosphorylation levels of TRPM7 by protein immunoprecipitated from lysates of mouse embryonic fibroblasts (MEF) using an anti-TRPM7 antibody. Autophosphorylation was clearly absent in mutant protein derived from TRPM7^{R/R} MEFs (Fig. 3, left panel). Phosphorylation of an exogenous substrate, myelin basic protein (MBP), was also abolished in these mice (Fig. 3, left panel). We confirmed the presence of similar levels of TRPM7 protein in immunoprecipitates from WT and TRPM7^{R/R} MEFs (Fig. 3, right panels).

TRPM7 channel activity in the TRPM7^{R/R} mutant macrophages. In our earlier study, which employed a heterologous expression system, we reported that channel function is not noticeably affected by knockdown of kinase activity¹⁵. In order to address the question whether TRPM7 channel activity is altered in TRPM7^{R/R} mice, we measured TRPM7 channel currents in peritoneal

macrophages derived from WT and TRPM7^{R/R} mice. RT-PCR experiments with specific primer sets for *Trpm7* and *Trpm6* showed that murine peritoneal macrophages expressed high levels of *Trpm7* but very little *Trpm6* (Fig. 4A, left panel). By contrast, kidney total RNA used as a positive control showed a strong TRPM6 signal as expected²⁵ (Fig. 4A, right panel). Kinase assay showed that TRPM7 kinase activity was compromised in TRPM7^{R/R} mutant macrophages (Fig. 4B), whereas protein levels were similar between WT and TRPM7^{R/R} mice (Fig. 4C). TRPM6 is the only other channel-kinase in the murine genome and its biophysical properties closely resemble TRPM7 at the whole-cell level²⁶, therefore it was important to ascertain that the cell type under investigation expresses primarily TRPM7 and not a mixture of TRPM6 and TRPM7. TRPM7 currents in macrophages have not been reported previously. Figure 4D shows the current-voltage relations obtained in WT and TRPM7^{R/R} mutant mouse peritoneal macrophages. The currents were evoked by depleting cytoplasmic Mg^{2+} with HEDTA-containing internal solution (free $[Mg^{2+}] = 400$ nM)¹². All WT macrophages tested exhibited robust TRPM7 currents with a characteristic outwardly rectifying current-voltage (I-V) curve (Fig. 4D, black). I-V was unchanged in the TRPM7^{R/R} mutant (Fig. 4D, red). In both WT and mutant macrophages currents developed with a similar time course (Fig. 4E) reaching a maximum after ~5 min of recording/dialysis with low- Mg^{2+} solutions. Current amplitudes measured at break-in (basal) were increased whereas the maximum current amplitudes were somewhat reduced in mutant macrophages (Fig. 4F, left). We therefore normalized the absolute current magnitudes to cell capacitances (Fig. 4F, right). Normalized maximum current densities were not significantly different between WT and TRPM7^{R/R} mutant macrophages, suggesting that the difference in absolute current stemmed from size variability of cells used in the recordings. Yet, unexpectedly, basal current densities showed significant potentiation in TRPM7^{R/R} macrophages. In order to ascertain that the currents measured in macrophages were indeed carried by TRPM7 channels, we examined the effects of internal high Mg^{2+} and spermine, known inhibitors of TRPM7 channels^{12,14}, as well as blockade of monovalent currents by external spermine¹. Inclusion of 303 μ M free Mg^{2+} or 300 μ M spermine in the pipette solution resulted in a drastic reduction of maximal current in both WT and kinase-dead macrophages, which was not statistically different (Fig. 4F). This concentration of Mg^{2+} was sufficient to inhibit basal TRPM7 currents in most cells. By contrast, in the presence of 300 μ M internal spermine, TRPM7 currents still developed but also ran down quickly (Suppl. Fig. 7B). We next compared the sensitivity of monovalent TRPM7 current in the absence of external Ca^{2+} to external spermine. The bathing solution was switched to DVF buffer to record monovalent TRPM7 current when the current achieved steady state amplitude with 400 nM internal Mg^{2+} and spermine was applied to the cell. Figure 4G shows I-V relations obtained in presence and immediately before application of 10 μ M spermine. In agreement with our previous report¹ we found that spermine preferentially blocked the inward component of monovalent TRPM7 current, displaying strong voltage dependence. The extent of spermine block did not significantly differ between WT and kinase-dead mutant macrophages (Fig. 4H). These experiments confirmed that the currents we recorded in murine macrophages mostly represent endogenous TRPM7 channel activity. We conclude therefore that TRPM7 channel activity is not significantly impaired when the C-terminus kinase is inactivated, in agreement with our previous findings¹⁵. Moreover, basal channel activity is higher when the kinase is inactivated.

Discussion

In this study, we generated TRPM7 kinase-dead mutant mice and analyzed the relationship between its kinase activity and channel

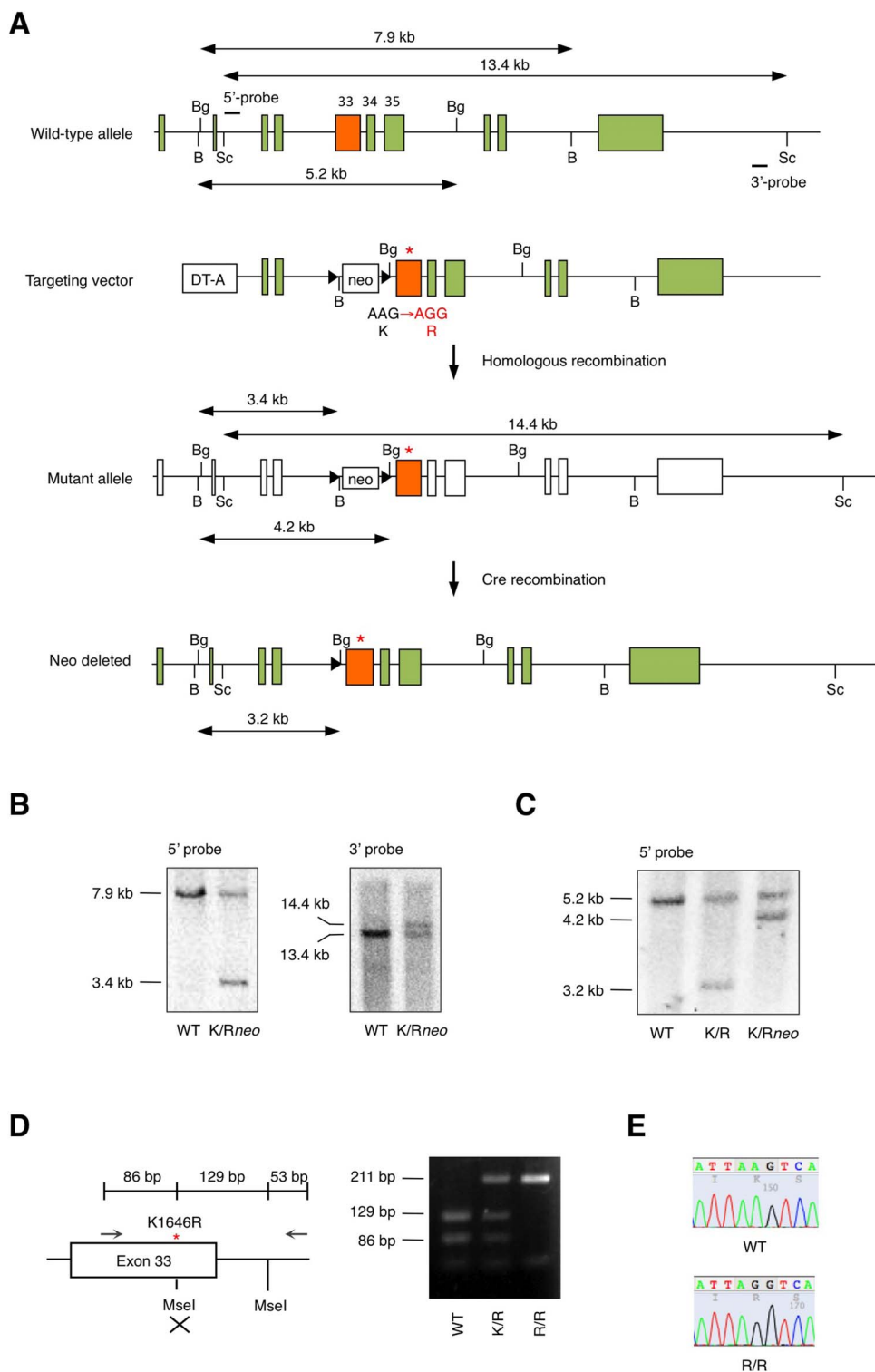


Figure 1 | Generation of TRPM7 kinase-dead knock-in mice. (A) Schematic diagram of the endogenous *Trpm7* locus and the targeting vector used to engineer embryonic stem (ES) cells by homologous recombination. This vector contains a point mutation in exon 33 that changes lysine residue at position 1646 to arginine (K1646R). Restriction enzyme sites are indicated (B, BamHI; Bg, BgIII; Sc, Scal). The length of the genomic fragment is also shown when digested by the indicated enzymes. Probes 5' and 3' were used to screen ES cells for homologous recombination by Southern blotting. DT-A, diphtheria toxin-A; neo, neomycin-resistant gene. (B) Southern blot analysis of genomic DNA from targeted ES cells using 5'-probe or 3'-probe after digestion with BamHI or Scal. Full length blots are shown in Fig. S1. (C) Southern blot analysis of genomic DNA from loxP-excised heterozygous mice using 5'-probe after digestion with BgIII. Full length blot is shown in Fig. S2. (D) PCR strategy used to genotype the animals. The region surrounding K1646R mutation was amplified by PCR and digested with MseI. A 211 bp fragment undigested at the mutated region is produced from wild-type (WT) allele, while the amplification product from the KR allele is digested into 129 bp and 86 bp fragments at the mutated region. PCR was performed on DNA isolated from tail biopsies; results from WT, TRPM7^{K/R}, and TRPM7^{R/R} animals are shown. Full length gel image is shown in Fig. S3. (E) PCR amplification products from WT and TRPM7^{R/R} animals were subcloned and sequenced to demonstrate the presence of the K1646R mutation; representative traces are shown.

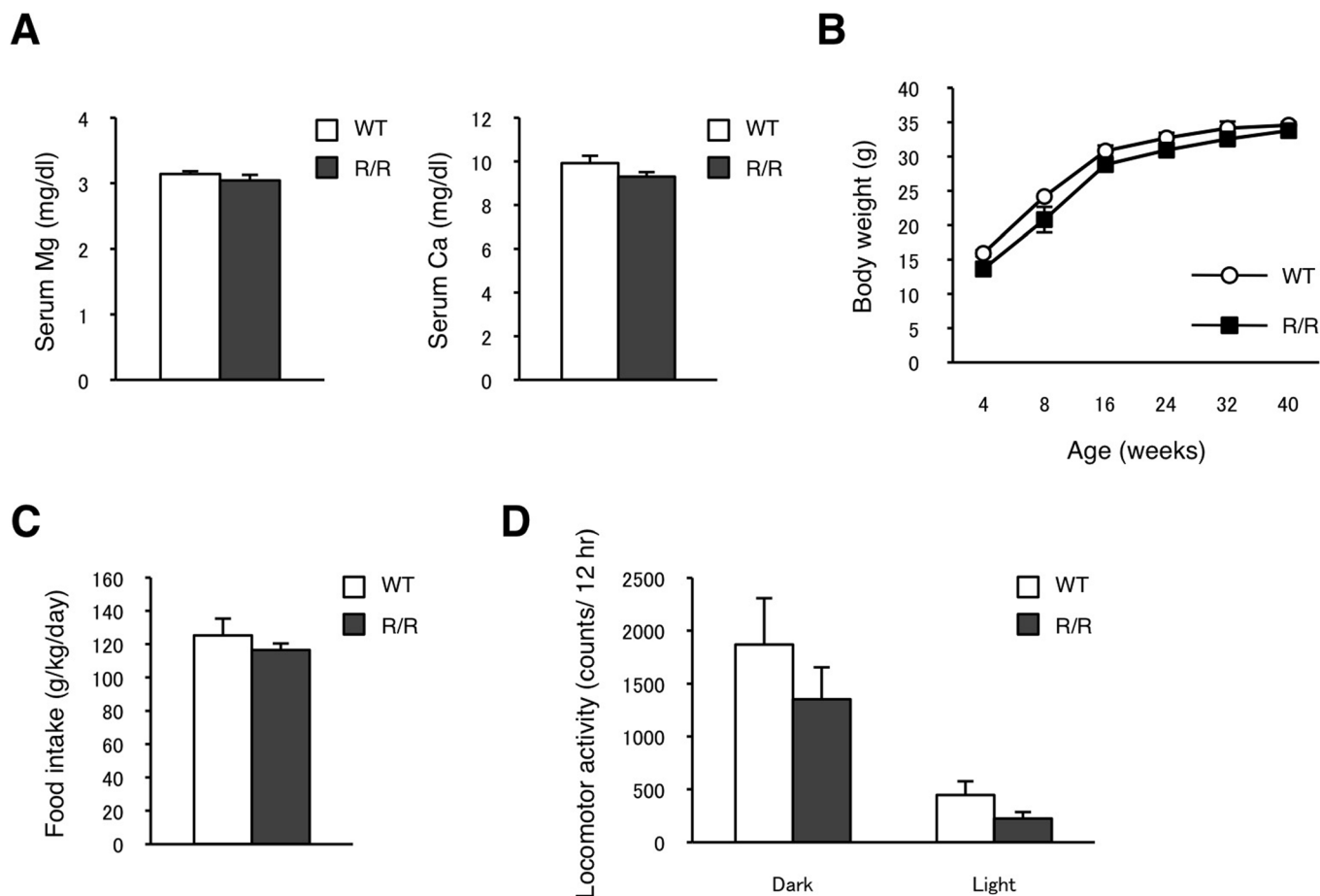


Figure 2 | Serum total Mg^{2+} and Ca^{2+} levels and general behaviors in $TRPM7^{R/R}$ mice. (A) Total Mg^{2+} and Ca^{2+} levels in serum obtained from WT and $TRPM7^{R/R}$ mice. Here and below values represent means \pm s.e.m. ($n = 10-14$). (B) Male WT and $TRPM7^{R/R}$ mice were weighed at the indicated times ($n = 6$). (C,D) General behavior was analyzed in 16 to 18 week-old WT and $TRPM7^{R/R}$ mice. (C) Food intake data. (D) Locomotor activity data ($n = 6$).

function. These mutant mice lacked any detectable kinase activity in their MEFs and macrophages. However, they exhibited normal serum Mg^{2+} and Ca^{2+} levels and developed normally. Furthermore, in macrophages isolated from $TRPM7^{R/R}$ mice, maximum channel activity was not affected by the absence of kinase activity. Interestingly, we find that basal TRPM7 channel activity, which represents their activity in an intact cell, was significantly potentiated.

TRPM7 is a member of the transient receptor potential (TRP) family of ion channels with a characteristic strong outward rectification and permeability to a number of divalent metal cations, including Mg^{2+} and Ca^{2+} ^{2,3}. TRPM7, and its closely related gene TRPM6 have key roles in Mg^{2+} homeostasis⁵⁻¹⁰. It was reported that deletion of TRPM7 in DT-40 chicken lymphoma cells arrests cell cycle progression⁸. Moreover, deletion of the entire mouse TRPM7 is lethal at embryonic day 7.5^{7,27}. Deletion of the kinase domain alone results in

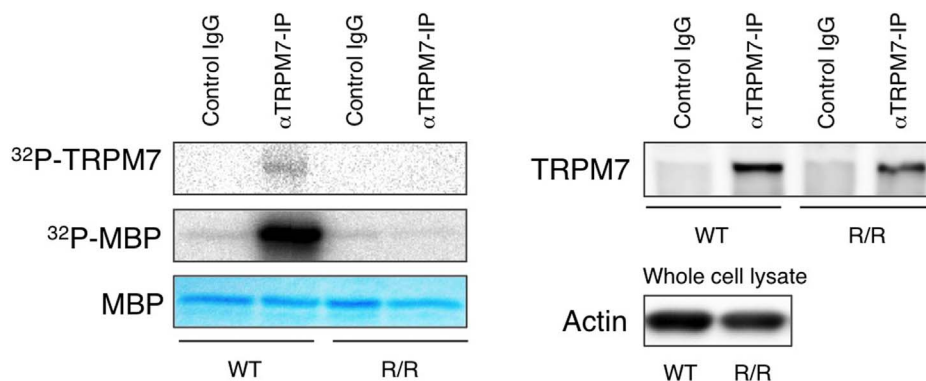


Figure 3 | TRPM7 kinase activity in $TRPM7^{R/R}$ mice. Kinase assay of TRPM7 proteins from WT and $TRPM7^{R/R}$ mouse embryonic fibroblasts (MEF). Left panel shows ^{32}P incorporation into autologous TRPM7 and exogenous myelin basic protein (MBP) by TRPM7 immunoprecipitated from WT or $TRPM7^{R/R}$ MEF lysates. Coomassie blue staining of MBP was used to ensure equal quantities of MBP. Right panel shows Western blot analysis of TRPM7 levels in the immunoprecipitates used in the left panel. Probing for actin in the whole cell lysates was used to ensure the presence of equal amount of protein in the lysates before immunoprecipitation. Full length blots and gel images are shown in Fig. S4.

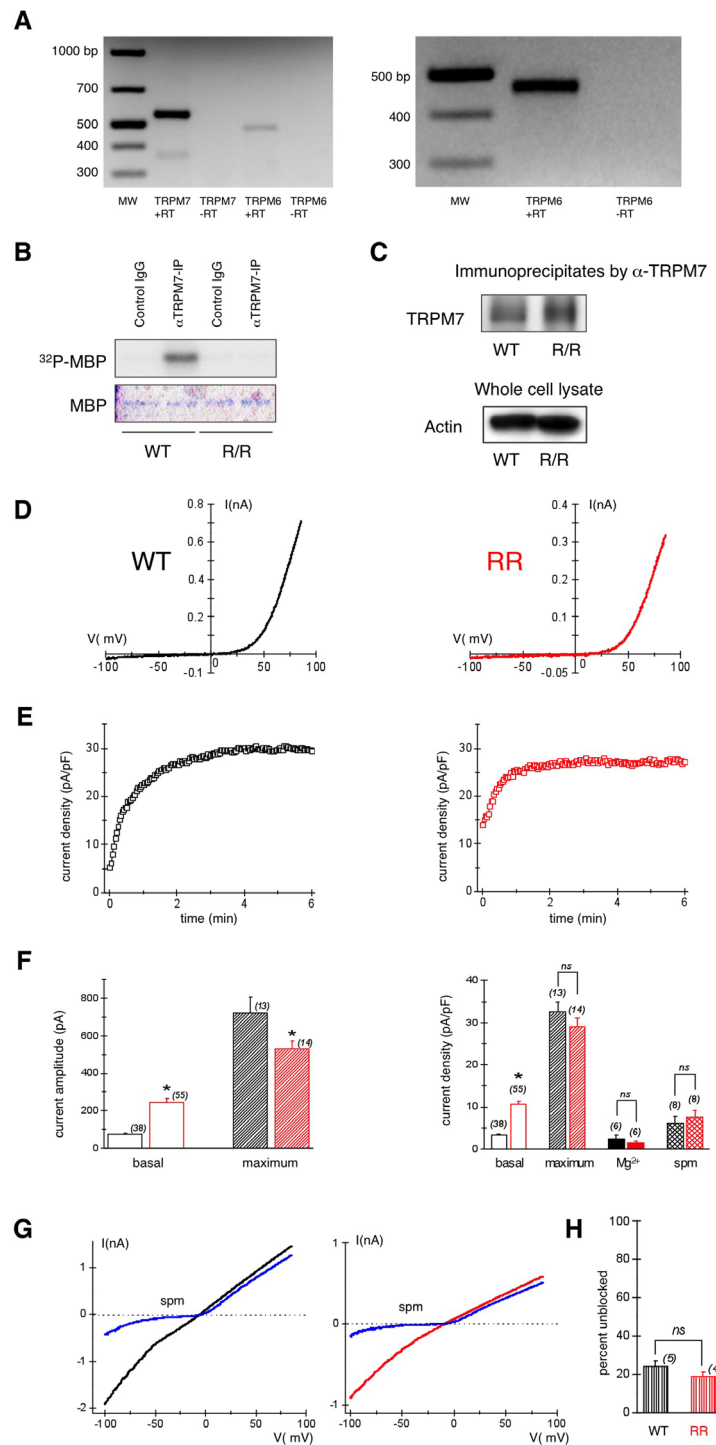


Figure 4 | TRPM7 channel and kinase activities in the macrophages of WT and TRPM7^{R/R} mice. (A) Expression of TRPM7 and TRPM6 mRNA in peritoneal macrophages. RT-PCR analysis of TRPM7 and TRPM6 expression in mouse peritoneal macrophages (left panel) and kidney (right panel). RT, reverse transcriptase. 40 and 38 cycles PCR were used for macrophage and kidney cDNA, respectively. Predicted TRPM7 size = 550 bp, predicted TRPM6 size = 475 bp. Full length gel images are shown in Fig. S5. (B) Kinase assay of TRPM7 protein isolated from peritoneal macrophages. ³²P incorporation into exogenous MBP by TRPM7 immunoprecipitated from lysates of WT or TRPM7^{R/R} macrophages is shown. Coomassie staining of MBP was used to ensure equal levels of MBP. Full length images are shown in Fig. S6. (C) Western blot analysis of TRPM7 in the immunoprecipitates used in (B). Actin in whole cell lysates was used to ensure the presence of equal protein amounts before immunoprecipitation. Full length gel images are shown in Fig. S7. (D) TRPM7 current-voltage relations recorded in WT (black) and TRPM7^{R/R} (red) peritoneal macrophages. (E) Time course of TRPM7 current development in the same cells. (F) Basal (break-in) and maximum TRPM7 current amplitudes (left) and densities (right) in WT and TRPM7^{R/R} mice. Internal solutions for measurement of basal and maximum currents contained 400 nM free Mg²⁺ (left). Internal Mg²⁺ and spermine solutions contained 303 μ M Mg²⁺ or 300 μ M spermine with no Mg²⁺ (E, right). Current amplitudes were obtained from the 125th ramp after break-in, $P < 0.01$ for basal, $P < 0.05$ for maximum. Time courses of current development with 300 μ M spermine are shown in Fig. S8. (G) Blockade of monovalent TRPM7 current by 10 μ M external spermine in macrophages isolated from WT (left) and kinase-dead mutant mice (right). (H) Percent unblocked monovalent TRPM7 current in WT and TRPM7^{R/R} mouse macrophages at -100 mV. Values are means \pm s.e.m. Numbers of cells are shown in parentheses.



early embryonic lethality in homozygous mice¹⁰. These results suggest that TRPM7 is essential for embryonic development and cell survival. In contrast, our present study demonstrates that the removal of TRPM7 kinase activity by point mutation does not affect cell growth and embryonic development, since TRPM7^{R/R} mice were born normally and weight gain was similar to WT mice. Both Schmitz et al. and Ryazanova et al. reported that deletion of the entire TRPM7 protein or the kinase domain disrupts Mg²⁺ homeostasis^{8,10}. In our TRPM7^{R/R} mice, the serum Mg²⁺ concentration was normal. This suggests that removal of kinase activity has little effect on Mg²⁺ homeostasis. This is supported by our findings in peritoneal macrophages, showing that the maximum number of functional TRPM7 channels is essentially the same in TRPM7^{R/R} mice. Ryazanova et al. reported that deletion of TRPM7 kinase domain significantly reduced TRPM7 channel activity in cells isolated from heterozygous mice¹⁰. This difference appears to be due to deletion of the kinase domain in full or in part¹⁰ vs. inactivation of phosphotransferase activity by point mutation (present study). The TRPM7 kinase domain plays a structural role and is essential for ion channel activity^{10,15}, and the absence of kinase domain was reported to alter TRPM7 channel sensitivity to Mg²⁺^{8,28}. Therefore, in these reports, deletion of the kinase domain seemed to lead to fatal deficits of TRPM7 channel function. Our results suggest, therefore, that embryonic lethality of kinase domain deletion¹⁰ is a consequence not of inactive kinase but rather of severely reduced ion channel function.

Runnels et al. showed that kinase activity regulates channel activity using heterologously expressed kinase-inactivated mutants in CHO-K1 cells¹⁶. Several reports also mentioned that kinase activity is related to channel function using kinase domain-deleted mutants^{8,10,23,28}. However, kinase domain has a structural role, and its deletion leads to not only deletion of kinase activity but also structural deficits¹⁵. Therefore, it has not been clarified whether kinase activity has a role in channel function. Here we show using knock-in strategy that deletion of kinase activity does not reduce maximal channel activity achieved with Mg²⁺ depletion. Unexpectedly, the basal activity of TRPM7 channels was increased. Basal channel activity reflects the portion of TRPM7 channels that are functional in an intact cell, before it is infused with low Mg²⁺ buffers. This pre-activation phenomenon was observed in other cell types (with presumably normal TRPM7 kinase function) and its nature is not known¹². In a heterologous expression system it is difficult to study channel pre-activation since overexpressed TRPM7 is always active whereas native TRPM7 is mostly inactive^{4,12,15,16}. It was previously reported that kinase-dead TRPM7 is less sensitive to inhibition by high Mg²⁺ (~2–8 mM)^{8,28}. Reduced Mg²⁺ sensitivity could lead to the larger pre-activated currents we observe (Fig. 4), however, 300 μM free Mg²⁺ was sufficient to inhibit basal TRPM7 currents in both WT and R/R macrophages equally, suggesting that cytoplasmic Mg²⁺, estimated to be in the range of 1–2 mM free, does not inhibit *all* TRPM7 channels. The reasons for this are not known and may include increased availability of PI(4,5)P₂ or increased sensitivity to this phospholipid in intact cells^{11,13,14}. The possibility that Mg²⁺ levels in kinase-dead mutant cells are significantly reduced causing greater channel activity cannot be ruled out although this seems unlikely in view of our finding that serum Mg²⁺ levels are not changed²⁷. Finally, we found a weak presence of TRPM6 channel-kinase in our RT-PCR experiments on WT macrophages (Fig. 4A), and it might play a role in facilitating TRPM7 basal activity²³. We did not detect single TRPM6 channel activity in macrophages, however (data not shown). Our future efforts will compare Mg²⁺ sensitivity of WT and R/R mutant TRPM7 channels in detail at the whole-cell and single-channel level, in view of the newly identified high affinity inhibitor site^{12,13}.

Several Mg²⁺ transporters are known to regulate cellular Mg²⁺ homeostasis, CNNM2, SLC41A1/2, Mrs2 and MagT1^{29–33}. TRPM7 kinase-dead mice exhibited normal levels of serum magnesium,

however, cellular Mg²⁺ levels in various tissues were not investigated. The possibility that TRPM7 kinase activity influences the function of these transporters and cellular Mg²⁺ levels cannot be excluded. We suggest that kinase activity is not essential for Mg²⁺ homeostasis and embryonic/adult mouse development, because kinase-dead mice did not show abnormal serum magnesium levels (i.e. hyper- or hypomagnesemia).

TRPM7 kinase is reported to have several substrates. Therefore, its kinase activity might have various physiological or pathophysiological roles in mammals. Our mutant mice, under standard conditions, developed normally and we did not observe any significant deficiencies. Further studies are needed for definition of the roles of TRPM7 kinase in physiology and pathophysiology.

Methods

Generation of TRPM7^{R/R} knock-in mice. A targeting vector was constructed to replace the exon 33 in *Trpm7* genomic locus with the DNA fragment containing a point mutation-inserted exon 33 (5'-AAG-3' to 5'-AGG-3') changing K1646 to R and loxP-flanked thymidine kinase promoter and neomycin resistance gene. This point mutation was generated by PCR and introduced into the targeting vector. A diphtheria toxin A fragment gene driven by MC-1 promoter was introduced at 5' end of the targeting vector. The linearized targeting vector was introduced into 129/SV ES cells by electroporation, and cells selected in G418. Genomic DNA from ES clones was screened for homologous recombination from both ends by Southern blot analysis using external probes 5'-probe and 3'-probe (Fig. 1A). Identified ES clone as targeted was injected into fertilized blastocysts from C57BL/6 female mice. Chimeric mice were mated with C57BL/6 female mice for germinal transmission. To excise the loxP-flanked neomycin cassette, fertilized eggs from C57BL/6 female paired with heterozygous mutant males were collected and pCAGGS-Cre was microinjected into the pronucleus²⁴. These eggs were then transferred into pseudopregnant mice and their offsprings were analyzed for excision of neomycin cassette by Southern blot. Heterozygous mice were backcrossed to C57BL/6 for at least seven generations. Homozygous mice (TRPM7^{R/R}) were obtained by intercrossing of heterozygous mice.

Experiments involving animals. All procedures involving mice were performed in compliance with the National Institutes of Health guidelines and were approved by the Laboratory Animal Care and Use Committees of Mitsubishi Kagaku Institute of Life Sciences, University of the Ryukyus, Kumamoto University and Wright State University.

For measurements of locomotor activity and food intake, the mice were acclimated to the single housing environment for 2 days, and locomotor activity data was collected with ACTIMO-100 (Shinfactory), and the food intake data was collected manually. Serum total Mg and Ca levels shown in Figure 2A were measured with an autoanalyzer (FUJI DRI-CHEM 3500 V, Fuji Film) at Skylight Biotech Inc. Mg was measured with FUJI DRI-CHEM SLIDE Mg-PIII (Fuji Film), and Ca was measured with FUJI DRI-CHEM SLIDE Ca-PIII (Fuji Film). These SLIDE-s detect both ionized and bound magnesium and calcium.

TRPM7 kinase assay. Mouse embryonic fibroblasts (MEFs) were obtained from WT or TRPM7^{R/R} mouse embryos. Peritoneal macrophages were isolated from adult mice³⁴. Cells were lysed in lysis buffer (50 mM Tris-HCl, pH 7.5, 120 mM NaCl, 0.5 mM DTT, 1.5 mM MgCl₂, 0.2 mM EDTA, 1% Triton X-100 supplemented with protease inhibitors) on ice for 20 min and insoluble materials were removed by centrifugation at 15,000 rpm for 10 min. Cell extracts were incubated with rabbit polyclonal anti-TRPM7 antibody (Millipore) overnight at 4°C, followed by incubation with protein A sepharose beads for 1 hr. Subsequently, the beads were washed three times in the lysis buffer and once in kinase buffer (50 mM HEPES, pH 7.0, 4 mM MnCl₂, 5 mM DTT). Immunoprecipitates were suspended in kinase buffer with 50 μg/ml myelin basic protein (MBP). The kinase reaction was initiated by adding 0.1 mM ATP in combination with 5 μCi [γ -³²P] ATP and proceeded for 30 min at 30°C. Proteins bound to the beads were eluted in Laemmli sample buffer, subjected to SDS-PAGE, and analyzed by autoradiography.

Isolation of peritoneal macrophages and RT-PCR. Peritoneal macrophages were isolated from WT or TRPM7^{R/R} mice of both sexes according to previous reports^{34,35}. Peritoneal cells were collected in Dulbecco's PBS containing 3% fetal bovine serum (FBS) through lavage of abdomen, and centrifuged at 1,500 r.p.m. for 8 min. The pellet was resuspended in RPMI medium and placed in cell culture dishes containing glass coverslips. After incubation for 1 hour at 37°C, the medium was replaced with RPMI containing 10% FBS, and attached cells were used for electrophysiological experiments and total RNA isolation. For RT-PCR experiments, Verso 1-step RT-PCR kit (Thermo Scientific) was used with RNA isolated from wildtype mouse macrophages and kidneys and forward and reverse primer pairs specific for murine TRPM7 GAATGGTCTGTGGAAAAGCACACG/CTTCTGCCCATACTTTCCAAC and TRPM6 GAGAGGAGGCCACAGTCAAG/CAGGCCCTGGTCACTG-TAAT.



Patch clamp electrophysiology. TRPM7 channel currents were recorded from murine peritoneal macrophages plated on glass coverslips using whole-cell patch clamp essentially as previously described^{11,12}. The basic internal solution contained (in mM) 10 HEDTA, 106 glutamic acid, 5 CsF, 8 NaCl, 10 HEPES and pH adjusted to 7.3 with CsOH. 60 μM MgCl_2 was added to this solution yielding estimated free $[\text{Mg}^{2+}]$ of 400 nM (Webmaxc software, Stanford University). For 303 μM free Mg^{2+} internal solution HEDTA and glutamic acid concentrations were reduced to 9 mM and 10 mM respectively and 7.74 mM MgCl_2 added. The standard external solution contained (in mM) 2 CaCl_2 , 140 NaAspartate, 4.5 KCl, 3 CsCl, 10 HEPES- Na^+ , 0.5 dextrose, pH 7.3. The divalent cation free external solution (DVF) contained (in mM) 140 NaAspartate, 6 HEDTA, 10 HEPES- Na^+ , pH 7.3^{11,13}. Macrophages have been reported to express substantial voltage-gated and inwardly rectifying K^+ currents^{35–37}. In order to record TRPM7 in isolation, the internal solution contained Cs^+ instead of K^+ and the external solution contained 3 mM CsCl to reduce K^+ channel contamination. Glutamate and aspartate were used as the main anions to reduce chloride conductances. For estimating external spermine block TRPM7 currents were allowed to develop to steady state with 400 nM free Mg containing internal solution, upon which the bathing solution was switched to DVF. Spermine was added to DVF¹. In experiments addressing internal 300 μM spermine inhibition, spermine tetrachloride was added to the 10 mM HEDTA internal solution. Cells were held at 0 mV and instantaneous current-voltage relations were obtained by applying -100 to $+85$ mV voltage ramps every 2.5 seconds. Voltage ramps were preceded by a 50 ms step to -100 mV. Time course of current development was plotted by taking current magnitudes measured at $+84.82$ mV and plotting against time. EPC10 patch clamp amplifier (HEKA Elektronik) operated by PatchMaster software was used for command voltage generation and data acquisition. Capillary glass from Warner Instruments was used to manufacture patch pipettes on a robotic Zeitz Universal puller or a vertical Narishige puller. Pipettes were fire polished to resistances of 3–5 mOhm using a Narishige MF830 microforge. Origin v. 8 (OriginLab) was used for data analysis and graphing. In Fig. 4F and H, two sample t-test was used to determine statistically significant differences between means. Osmolalities were adjusted with D-mannitol. All experiments were performed at room temperature ($\sim 25^\circ\text{C}$).

- Kozak, J. A., Kerschbaum, H. H. & Cahalan, M. D. Distinct properties of CRAC and MIC channels in RBL cells. *J. Gen. Physiol.* **120**, 221–235 (2002).
- Nadler, M. J. *et al.* LTRPC7 is a Mg-ATP-regulated divalent cation channel required for cell viability. *Nature* **411**, 590–595 (2001).
- Monteilh-Zoller, M. K., Hermosura, M. C., Nadler, M. J., Scharenberg, A. M., Penner, R. & Fleig, A. TRPM7 provides an ion channel mechanism for cellular entry of trace metal ions. *J. Gen. Physiol.* **121**, 49–60 (2003).
- Gwanyanya, A. *et al.* Magnesium-inhibited, TRPM6/7-like channel in cardiac myocytes: permeation of divalent cations and pH-mediated regulation. *J. Physiol.* **559** (Pt 3), 761–776 (2004).
- Schlingmann, K. P. *et al.* Hypomagnesemia with secondary hypocalcemia is caused by mutations in TRPM6, a new member of the TRPM gene family. *Nat. Genet.* **31**, 166–170 (2002).
- Walder, R. Y. *et al.* Mutation of TRPM6 causes familial hypomagnesemia with secondary hypocalcemia. *Nat. Genet.* **31**, 171–174 (2002).
- Brandao, K., Deason-Towne, F., Perraud, A. L. & Schmitz, C. The role of Mg^{2+} in immune cells. *Immunol. Res.* **55**, 261–269 (2013).
- Schmitz, C. *et al.* Regulation of vertebrate cellular Mg^{2+} homeostasis by TRPM7. *Cell* **114**, 191–200 (2003).
- Chubanov, V. *et al.* Disruption of TRPM6/TRPM7 complex formation by a mutation in the TRPM6 gene causes hypomagnesemia with secondary hypocalcemia. *Proc. Natl. Acad. Sci. U. S. A.* **101**, 2894–2899 (2004).
- Ryazanova, L. V. *et al.* TRPM7 is essential for Mg^{2+} homeostasis in mammals. *Nat. Commun.* **1**, 109 (2010).
- Gwanyanya, A., Sipido, K. R., Vereecke, J. & Mubagwa, K. ATP and PIP_2 dependence of the magnesium-inhibited, TRPM7-like cation channel in cardiac myocytes. *Am. J. Physiol. Cell Physiol.* **291**, C627–635 (2006).
- Chokshi, R., Matsushita, M. & Kozak, J. A. Detailed examination of Mg^{2+} and pH sensitivity of human TRPM7 channels. *Am. J. Physiol. Cell Physiol.* **302**, C1004–1011 (2012).
- Chokshi, R., Matsushita, M. & Kozak, J. A. Sensitivity of TRPM7 channels to Mg^{2+} characterized in cell-free patches of Jurkat T lymphocytes. *Am. J. Physiol. Cell Physiol.* **302**, C1642–1651 (2012).
- Kozak, J. A., Matsushita, M., Nairn, A. C. & Cahalan, M. D. Charge screening by internal pH and polyvalent cations as a mechanism for activation, inhibition, and rundown of TRPM7/MIC channels. *J. Gen. Physiol.* **126**, 499–514 (2005).
- Matsushita, M. *et al.* Channel function is dissociated from the intrinsic kinase activity and autophosphorylation of TRPM7/ChaK1. *J. Biol. Chem.* **280**, 20793–20803 (2005).
- Runnels, L. W., Yue, L. & Clapham, D. E. TRP-PLIK, a bifunctional protein with kinase and ion channel activities. *Science* **291**, 1043–1047 (2001).
- Yamaguchi, H., Matsushita, M., Nairn, A. C. & Kuriyan, J. Crystal structure of the atypical protein kinase domain of a TRP channel with phosphotransferase activity. *Mol. Cell* **7**, 1047–1057 (2001).
- Drennan, D. & Ryazanov, A. G. Alpha-kinases: analysis of the family and comparison with conventional protein kinases. *Prog. Biophys. Mol. Biol.* **85**, 1–32 (2004).

- Nairn, A. C. *et al.* Elongation factor-2 phosphorylation and the regulation of protein synthesis by calcium. *Prog. Mol. Subcell. Biol.* **27**, 91–129 (2001).
- Dorovkov, M. V., Kostyukova, A. S. & Ryazanov, A. G. Phosphorylation of annexin A1 by TRPM7 kinase: a switch regulating the induction of an α -helix. *Biochemistry* **50**, 2187–2193 (2011).
- Deason-Towne, F., Perraud, A. L. & Schmitz, C. Identification of Ser/Thr phosphorylation sites in the C2-domain of phospholipase $\text{C}\gamma 2$ (PLC $\gamma 2$) using TRPM7-kinase. *Cell Signal.* **24**, 2070–2075 (2012).
- Perraud, A. L., Zhao, X., Ryazanov, A. G. & Schmitz, C. The channel-kinase TRPM7 regulates phosphorylation of the translational factor eEF2 via eEF2-k. *Cell Signal.* **23**, 586–593 (2011).
- Zhang, Z. *et al.* The TRPM6 kinase domain determines the Mg ATP-sensitivity of TRPM7/M6 heteromeric ion channels. *J. Biol. Chem.* **289**, 5217–5227 (2014).
- Kitamoto, T. *et al.* Humanized prion protein knock-in by Cre-induced site-specific recombination in the mouse. *Biochem. Biophys. Res. Commun.* **222**, 742–747 (1996).
- Bödding, M. TRPM6: A Janus-like protein. *Handb. Exp. Pharmacol.* **179**, 299–311 (2007).
- Topala, C. N. *et al.* Molecular determinants of permeation through the cation channel TRPM6. *Cell Calcium* **41**, 513–523 (2007).
- Jin, J., Desai, B. N., Navarro, B., Donovan, A., Andrews, N. C. & Clapham, D. E. Deletion of *Trpm7* disrupts embryonic development and thymopoiesis without altering Mg^{2+} homeostasis. *Science* **322**, 756–760 (2008).
- Demeuse, P., Penner, R. & Fleig, A. TRPM7 channel is regulated by magnesium nucleotides via its kinase domain. *J. Gen. Physiol.* **127**, 421–434 (2006).
- Stuiver, M. *et al.* CNNM2, encoding a basolateral protein required for renal Mg^{2+} handling, is mutated in dominant hypomagnesemia. *Am. J. Hum. Genet.* **88**, 333–343 (2011).
- Wabakken, T., Rian, E., Kveine, M. & Aasheim, H. C. The human solute carrier SLC41A1 belongs to a novel eukaryotic subfamily with homology to prokaryotic MgtE Mg^{2+} transporters. *Biochem. Biophys. Res. Commun.* **306**, 718–724 (2003).
- Goytain, A. & Quamme, G. A. Functional characterization of the mouse solute carrier, SLC41A2. *Biochem. Biophys. Res. Commun.* **330**, 701–705 (2005).
- Zsurka, G., Gregán, J. & Schweyen, R. J. The human mitochondrial Mrs2 protein functionally substitutes for its yeast homologue, a candidate magnesium transporter. *Genomics* **72**, 158–168 (2001).
- Goytain, A. & Quamme, G. A. Identification and characterization of a novel mammalian Mg^{2+} transporter with channel-like properties. *BMC Genomics* **6**, 48 (2005).
- Martinez-Pomares, L. & Gordon, S. Murine macrophages: a technical approach. *Methods Mol. Biol.* **415**, 255–272 (2008).
- Ypey, D. L. & Clapham, D. E. Development of a delayed outward-rectifying K^+ conductance in cultured mouse peritoneal macrophages. *Proc. Natl. Acad. Sci. U. S. A.* **81**, 3083–3087 (1984).
- Randriampita, C. & Trautmann, A. Ionic channels in murine macrophages. *J. Cell Biol.* **105**, 761–769 (1987).
- Gallin, E. K. Ion channels in leukocytes. *Physiol. Rev.* **71**, 775–811 (1991).

Acknowledgments

We thank Rikki Chokshi, Urszula Osinska, Sai Kolipara for excellent technical assistance and Mark Rich for useful comments on the manuscript. This research was funded by Japanese Ministry of Education, Culture, Sports, Science and Technology (MM), The Promotion Project of Medical Clustering of Okinawa Prefecture (MM) and American Heart Association, National Center (JAK). SH was supported in part by GM090122 NIGMS R25 grant.

Author contributions

T.K., C.K. and M.M. designed experiments. T.K. and C.K. performed most of the experiments, P.B., S.H. and J.A.K. designed and carried out electrophysiological analysis and RT-PCR experiments. K.N. supported the generation of knock-in mice. K.T. provided critical advice. T.K., C.K., J.A.K. and M.M. wrote the paper.

Additional information

Supplementary information accompanies this paper at <http://www.nature.com/scientificreports>

Competing financial interests: The authors declare no competing financial interests.

How to cite this article: Kaitsuka, T. *et al.* Inactivation of TRPM7 kinase activity does not impair its channel function in mice. *Sci. Rep.* **4**, 5718; DOI:10.1038/srep05718 (2014).



This work is licensed under a Creative Commons Attribution-NonCommercial-ShareAlike 4.0 International License. The images or other third party material in this article are included in the article's Creative Commons license, unless indicated otherwise in the credit line; if the material is not included under the Creative Commons license, users will need to obtain permission from the license holder in order to reproduce the material. To view a copy of this license, visit <http://creativecommons.org/licenses/by-nc-sa/4.0/>